Available online at www.sciencedirect.com

SCIENCE DIRECT®

Tectonophysics 388 (2004) 21–31

TECTONOPHYSICS

www.elsevier.com/locate/tecto

Thermo-mechanical structure beneath the young orogenic belt of Taiwan

Kuo-Fong Ma*, Teh-Ru Alex Song[1]

Department of Earth Sciences, National Central University, 300 Jungda Road, Chung-Li, 320-54 Taiwan, ROC

Received 11 July 2003; received in revised form 29 January 2004; accepted 13 June 2004

Abstract

We investigate the thermo-mechanical properties beneath the young orogenic belt of Taiwan by constructing a shear strength profile from a vertical stratified rheological structure. The stratified rheological structure is estimated based on the recently developed thermal structure and its likely composition. Subduction–collision in the young orogenic belts and the thick accretionary wedge make a significant contribution to the growth of sialic crust in the hinterland. The sialic bulk crust not only results in a low seismic velocity but also produces weak crust in the hinterland. The earthquake depth–frequency distribution in the foreland and hinterland correlates very well with the regimes of the brittle/ductile transition revealed in the strength profile. Our results show that the observed two-layer seismicity in the foreland is due to a moderate geotherm and an intermediate mafic bulk composition; while single-layer seismicity in the hinterland is due to its felsic bulk composition. In the foreland, the mechanically strong crust (MSC) and the mechanically strong lithosphere (MSL) coincide with frequent seismicity. The shallow MSC in the hinterland is consistent with the 20- to 25-km seismicity occurring there. The total lithospheric integrated strength (LIS) in the hinterland is only about half of that in the foreland, suggesting a weak lower crust and lithosphere mantle in the hinterland. The results confirm that the earthquake cutoff depth is a proxy for temperature. The calculated decrease of effective elastic thickness (EET) from the orogenic margin (foreland) to the center (hinterland) is consistent with the results of flexure modeling in most orogenic belts. Due to the weak LIS in the hinterland, crustal thinning and rifting may occur in the future. Our results, thus, suggest that the mechanical structure is also closely related to the composition and is not directly reflected in the thermal structure.

Keywords: Thermo-mechanical; Rheology; Seismicity; Strength profile; Composition

1. Introduction

A mechanical structure of the lithosphere in the active arc–continent collision zone of Taiwan is essential for understanding observed seismicity. The seismicity of the arc–continent collision region of Taiwan is due to its tectonic setting within the

* Corresponding author. Tel.: +886 3 4262421; fax: +886 3 4222044.

E-mail address: fong@earth.ncu.edu.tw (K.-F. Ma).

[1] Present address: Seismological Laboratory, California Institute of Technology, USA.

0040-1951/$ - see front matter © 2004 Elsevier B.V. All rights reserved.
doi:10.1016/j.tecto.2004.07.003

collision of the Philippine Sea and Eurasian Plates, as shown in Fig. 1. The Taiwan mountain ranges are composed of the exhumed Eurasian Paleozoic to Mesozoic metamorphic basement within the Eastern Central Range (ECR), Neogene to Paleogene slate belts in the Backbone Range (BR), and the Hsueshan Range (HR) in the Central Range. Further to the west, a typical foreland fold and thrust belt, the Western Foothills (WF) and the concentration of active faults in the Western Plain (WP) occur. Fig. 2 shows the seismicity recorded by the Central Weather Bureau Seismic Network (CWBSN) for events with M>2 and depth <50 km for the time period of 1973–1997. In the center of the foreland, a region of low seismicity activity was found, which correlates closely with the position of the Peigang (PG) basement high, a major

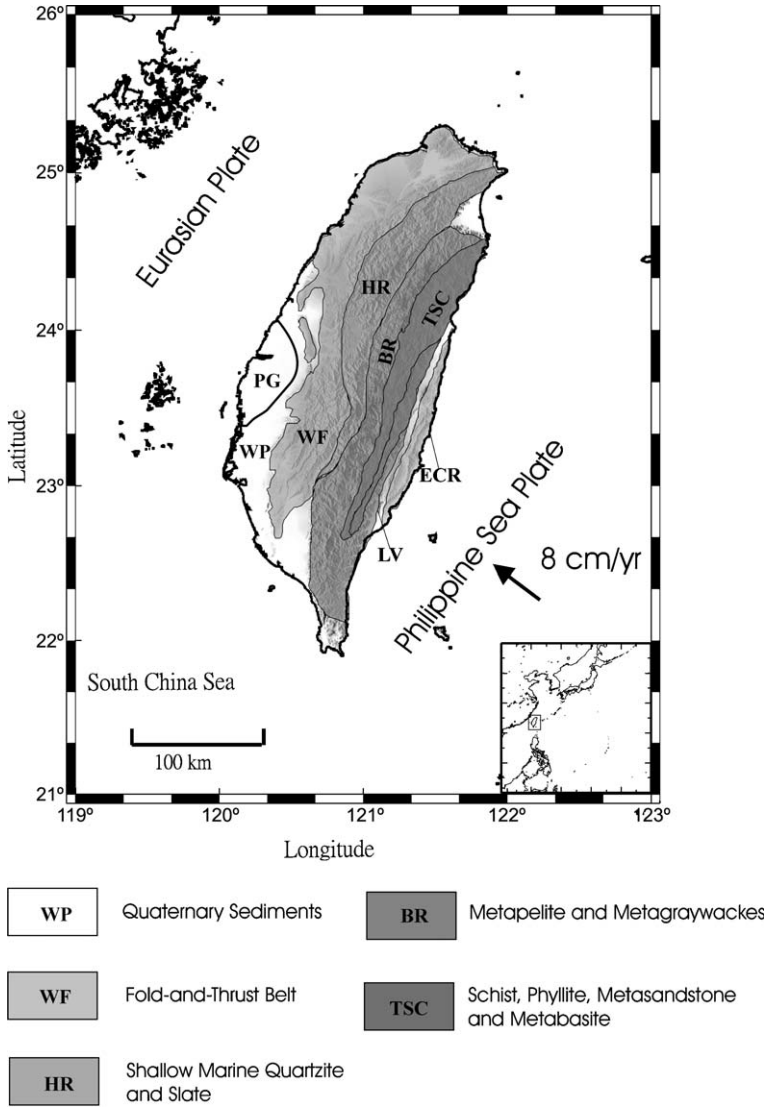

Fig. 1. Plate tectonic setting at the Eurasian/Philippine Sea boundary and the arc–continent collision at Taiwan. The prominent geological features are represented. PG: Peigang high; WP: West Plain as Quaternary sediments; WF: West Foothill as fold-and-thrust belt; HR: Hsueshan Range as shallow marine quartzite and slate; BR: Backbone Range as metapelite and metagraywackes; TSC: Tanano schist as schist, phyllitem metasandstone, and metabasite; ECR: East Coastal Range; and LV: Longitudinal Valley.

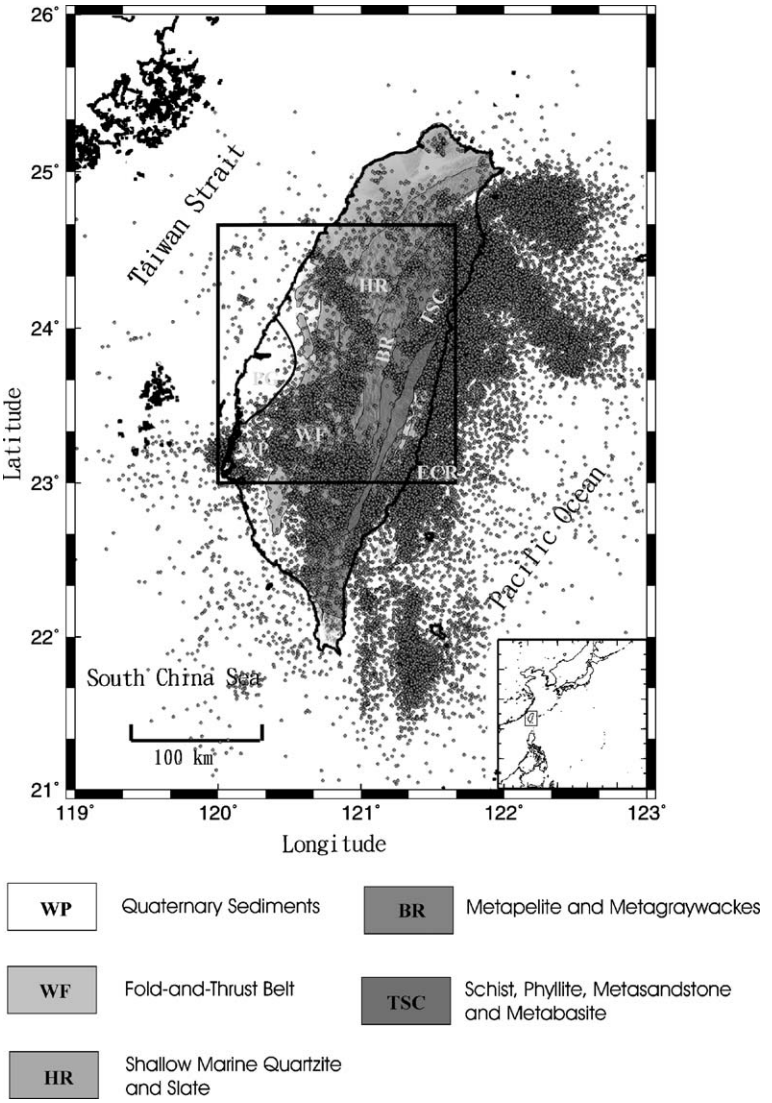

Fig. 2. Seismicity recorded by the CWBSN for events with M>2 and depth <50 km for the time period of 1973–1997. The box indicates the studied region.

inherited feature of the Chinese margin. Except for the seismicity in PG, the level of seismicity in the hinterland (HR and BR) is low compared to that in the foreland (WF and WP). The statistics for the earthquake frequency (M>5)–depth (<50 km) distribution, as shown in Fig. 3 for the foreland and hinterland, clearly depicted two-layer seismicity in the foreland. The upper layer is mainly at a depth of 5–15 km and the lower one is at a depth of 25–40 km. In the hinterland, most events are limited to the upper 15 km of the crust. Below the depth of 25 km, less seismicity is observed. The seismicity data have been extensively investigated to understand the earthquake–frequency relationship as it relates to the tectonic setting (Wang et al., 1994), and the depth–frequency distribution to the rheological structure (Wu et al., 1997). Wang et al. (1994) suggested that a high geothermal gradient might be the dominating factor of the low seismicity in the lower crust of the hinterland. Wu et al. (1997) interpreted that the two-layer

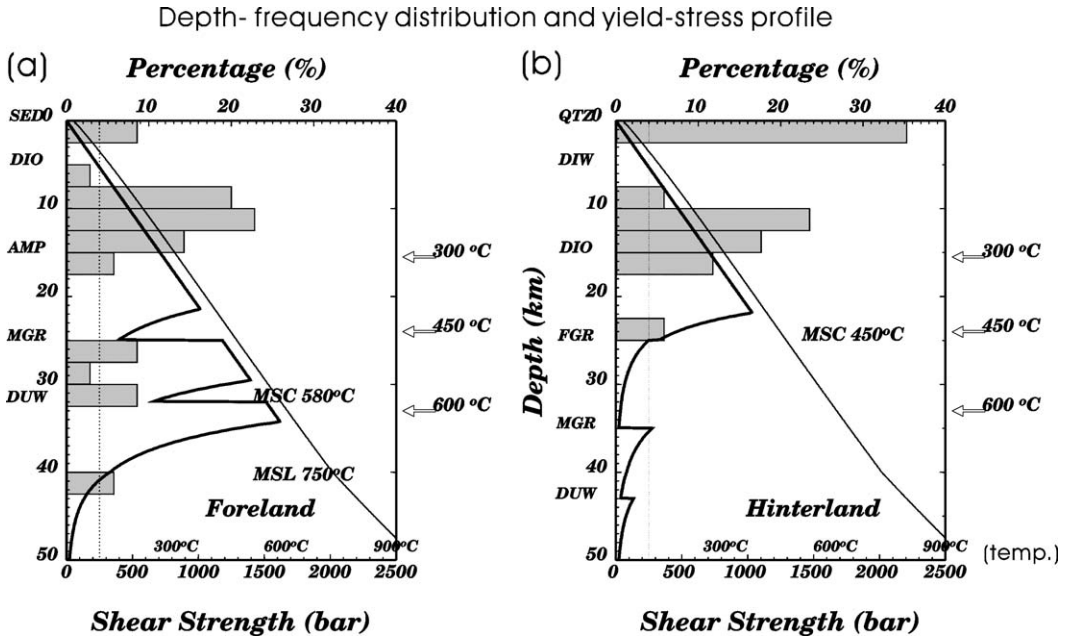

Fig. 3. Earthquake depth–frequency distribution and shear strength profile in (a) foreland and (b) hinterland. The average temperature profile is also shown for reference. The RRs (Fig. 4) at the corresponding depth for both foreland and hinterland are also shown. The dashed line indicates the strength of 250 bar, which represents the lower bound of the MSC and the MSL. The MSC and MSL indicated in the figure represent their corresponding bottom depths and temperatures.

seismicity in the foreland probably corresponds to the two brittle layers induced by the occurrences of quartz and olivine. They also explained the low seismicity in the lower crust in the hinterland by high temperature. Due to a lack of information on composition and thermal structure within the crust, no specific stratified rheological structure was constructed in the work of Wu et al. (1997).

The study of the thermo-mechanical structure of Okaya et al. (1996) shows that no direct correlation between surface heatflow and total strength of the crust. The surface heatflow values are too uncertain to constrain the predicted surface heatflow. Song and Ma (2002) estimated the 1-D thermal structure of Taiwan by assuming crustal thickening followed by a constant erosional process. Their results predicted a moderate geothermal gradient (20–25 °C/km) in the hinterland, after excluding the observed heatflows (Lee and Cheng, 1986), which are accounted for by the effect of groundwater circulation. Thus, except for the easternmost hinterland (TSC), which belongs to a rapid-uplift region due to crustal exhumation after the subduction of the continental margin (Lin, 2000), no significant geothermal differences occur between the foreland and hinterland. Lin (2000) also suggested that the occurrence of deeper earthquakes east of the Central Range (TSC) is a result of the lower thermal gradient, which is due to the subduction of the cold continental crust into the uppermost mantle. Based on the tomographic images of Ma et al. (1996), the crustal composition derived from tomographic velocities and laboratory data (Christensen and Mooney, 1995; Rudnick and Fountain, 1995) suggests that the hinterland is composed of a felsic bulk crust, while the foreland is of intermediate mafic bulk crust. This possible crustal composition difference might have some influence on the level of seismicity within the Taiwan orogenic belts. Using the thermal structure and possible composition, we constructed a vertical stratified rheological structure, in which the strength varies with depth, to investigate its correlation with seismicity. The rheological stratifications are further examined to estimate the corresponding lithospheric strength, effective elastic thickness (EET), mechan-

ically strong crust (MSC), and lithosphere in the foreland and hinterland, and to understand the thermo-mechanical structure beneath the young orogenic belt of Taiwan. These thermo-mechanical parameters provide important insights into the coupling/decoupling of the crust and mantle, and thus the strength of the lithosphere. Both of the factors are useful for a better understanding of the mountain building process within the Taiwan Orogeny.

2. Shear strength profile and rheological model

We calculated lithospheric shear strength profiles based on a simple brittle/ductile model. The brittle shear strength is expressed as (Sibson, 1974):

$$\tau_b = \frac{1}{2}\beta\rho g h(1-\lambda) \quad (1)$$

where τ_b is brittle shear strength; β is a constant, which is related to fault type and frictional coefficient; ρ is density; g is the acceleration of gravity; h is depth; and λ is pore pressure ratio. The ductile shear strength is described by the power-law creep equation as (e.g., Ranalli and Murphy, 1987):

$$\tau_d = \frac{1}{2}\left[\left(\frac{\dot{\varepsilon}}{B}\right)^{1/2}\exp\left(\frac{E}{nRT}\right)\right] \quad (2)$$

where τ_d is ductile shear strength, $\dot{\varepsilon}$ is strain rate (s^{-1}), R is the gas constant, T is absolute temperature (K), and B, n, and E are material constants. At the same depth, lithospheric shear strength represents the smallest of the brittle shear strength and the ductile shear strength. In this study, λ is taken as 0.4, and the average density is 2800 kg/m^3. Based on the surface geology (Ho, 1988), the fault type is given as wrench faulting for Taiwan region. These assumptions are somewhat arbitrary, but this has no significant effect on the shear strength patterns (e.g., Sibson, 1984). The brittle shear strength is significantly reduced along the preexisting faults, fault gouges, and fractures that are broadly distributed in Taiwan orogenic belts (Ho, 1988). In addition, considering the possible limitation of the maximum lithospheric shear strength of 1 kbar (Lamontagne and Ranalli, 1996) and the existence of high-angle faults underneath Taiwan (Rau et al., 1996), we adopted a frictional coefficient of 0.3 (Lamontagne and Ranalli, 1996), instead of 0.75 in general, to represent these weak lithologies and reactivated high-angle faults within the active orogenic belts. The temperature profile used in the calculation of ductile shear strength is based on the geotherm derived by Song and Ma (2002). As delineated in Song and Ma (2002), the temperature difference between the foreland and hinterland is about 100 °C at the bottom of the crust, but this merely influences the location of brittle/ductile transition, not the strength pattern, namely, single brittle shear strength peak or double peaks. We considered strain rate of about 10^{-14} s^{-1} from global positioning system (GPS) measurements (Yu and Chen, 1994) and seismic moment tensor results (Kao et al., 1998).

The rheological model was based on the composition beneath Taiwan. The composition beneath Taiwan, as a product of late Cenozoic orogenic belts, is poorly understood due to its complex tectonic structure. Recent tomographic results from a dense seismic network and high-quality seismic data provide important information on the crustal structure of Taiwan. This tomographic velocity structure might not be as detailed as the field refraction data, but it is still significant in providing the velocity structure of deeper crust. A comparison between observed seismic velocities and those measured in the laboratory (Christensen and Mooney, 1995) gives an indication of the composition of the crust. The crustal composition was based on the geology of the Taiwan orogenic belts. Instead of specific rock type, V_p was correlated with general lithologic categories to avoid the ambiguity. The V_p/V_s ratio derived from a reliable S-wave velocity of tomographic inversion was also considered as a constraint on the crustal composition. From tomography P-wave velocity and V_p/V_s ratio, a felsic bulk crust in the hinterland and mafic bulk crust in the foreland were derived for the Taiwan orogenic belts. The derived composition was also compared with a different dataset compiled by Rudnick and Fountain (1995) for further justification. Regardless of the existence of some differences in the detail constituents between the two physical properties datasets, the felsic bulk crust for the hinterland remains true.

The derived composition was further examined by surface geology and xenoliths. The SiO_2 content of the derived composition is in good agreement with the

geochemical study on metapelites (Youh and Tan, 1975; Chen et al., 1984). Considering that the hinterland may be an accretionary wedge due to subduction–collision orogenic event (Teng, 1990; Lu and Hsu, 1992), one would expect that much more marine sediments and sialic materials of the upper crust might be subducted into the deeper crust. Most of these materials would undergo regional metamorphism, transforming into felsic–metamorphic rocks and making up the bulk composition of the lower crust (Meissner, 1986). Thus, the result of a felsic bulk composition (such as mica–quartz schist, felsic granulite, paragranulite, and paragneiss) for the middle–lower crusts (at 20 and 30 km) in the hinterland is not unexpected. There are no geological data available for the deep crust of the foreland. However, mafic granulite xenoliths investigated in the southeast China continental margin by Lee et al. (1994) may give information concerning the composition of the lower crust (20–35 km) in this region. The SiO_2 content of these mafic granulite xenoliths is in the range 48–52%, which is in reasonable agreement with that of about 45–55% for the lower crust in WP found in the composition study. On the basis of the observed P-wave velocity, V_p/V_s ratio, surface geology, and xenoliths as discussed above, it is concluded that the bulk crustal composition in the hinterland is more felsic than that in the foreland. The sialic bulk crust not only corresponds to the low seismic velocity but also produces a weak crust in the hinterland. The felsic young crust might be rifted because of weak crustal integrated strength and convective thinning due to the gravitational instability.

On the basis of the derived crustal compositions, we constructed a six-layer rheological model as shown in Fig. 4. These stratifications are designed to correspond to the divisions of layers from tomography image (Ma et al., 1996). Moho depth is chosen as 32 km in the foreland and 43 km in the hinterland from the Pn study (Ma and Song, 1997) and reflection experiments (Shih et al., 1998). Flow parameters corresponding to the rheological stratifications are listed in Table 1. Based on the surface geology (Ho, 1988), a first layer (0–5 km) of sediments for the foreland and wet quartzites for the hinterland are taken as the "representative rocks" (RRs). RRs might not be exactly the constitutions in the crust, but they most closely resemble the actual crustal physical properties in the present data set. Considering the scarcity of information on flow parameters for some metamorphic rocks, like gneiss, schist, and slate, and the relevant SiO_2 content in the crust, we take wet quartz diorite as RRs for the depth range of 5–15 km. For the same reason, dry quartz

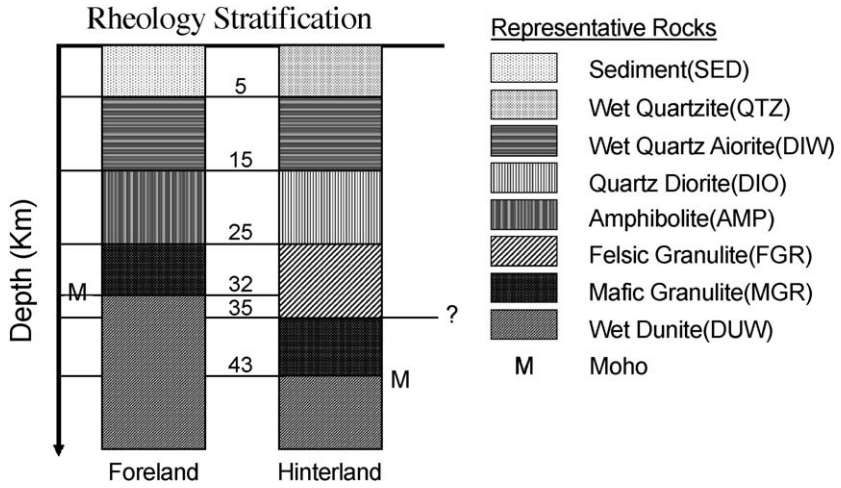

Fig. 4. Vertical rheology stratification for foreland and hinterland. The RRs are sediments (SED), wet quartz diorite (DIW), amphibolite (AMP), mafic granulite (MGR), and wet dunite (DUW) for the foreland; wet quartzite (QTZ), quartz diorite (DIO), felsic granulite (FGR), mafic granulite (MGR), and wet dunite (DUW) for the hinterland. The Moho depths are at 32 and 43 km, respectively, for the foreland and hinterland.

Table 1
Flow parameters for the RRs adopted for computation of shear strength profile

RRs	Flow parameters		
	n	E (kJ/mol^{-1})	B (MPa^{-n}s^{-1})
Sediment (SED)	3	190	5.00×10^{-6}
Wet quartzite (QTZ)	1.9	173	3.16×10^{-2}
Wet quartz diorite (DIW)	2.4	219	3.80×10^{-2}
Quartz diorite (DIO)	2.4	219	1.30×10^{-3}
Amphibolite (AMP)	3.7	244	1.70×10^{-4}
Felsic granulite (FGR)	3.1	243	8.00×10^{-3}
Mafic granulite (MGR)	4.2	445	1.40×10^{4}
Wet dunite (DUW)	4	471	2.00×10^{3}

Data from Doser and Kanamori (1986), Ranalli (1995), and Okaya et al. (1996).

diorite is adopted for the depth range of 15–25 km in the hinterland. In the foreland, amphibolite is adopted at this layer. Considering the crustal composition, mafic granulite is considered as the RR between 25 km and Moho depth in the foreland. In the hinterland, felsic granulite and mafic granulite are considered as RRs at the depth of 25–35 km 35 km to Moho, respectively. For depths greater than the Moho discontinuity, wet dunite is assumed.

On the basis of the constructed rheological model, lithospheric shear strength profiles for the Taiwan orogenic belts are derived and shown in Fig. 3 along with the earthquake frequency (M>5)–depth distribution. It is apparent that seismicity distribution is relatively consistent with the occurrence of brittle layers. The nearly aseismic zone is probably due to the ductile deformation. The three brittle layers in the foreland are attributed to the constitution of quartz (300 °C isotherm), feldspar (450 °C isotherm), and dunite (600 °C isotherm). Only a single brittle layer is found in the hinterland due to its felsic bulk composition, moderate geotherm gradient, and thick crust. These specific characteristics in the hinterland are directly responsible for the regional low seismicity in the lower crust. In general, the earthquake depth distributions and brittle regimes are well correlated beneath Taiwan orogenic belts.

3. Mechanical structure in Taiwan orogenic belts

From shear strength profiles, several mechanical parameters could be derived, such as integrated lithospheric strength (ILS), MSC, mechanically strong lithosphere (MSL), and EET. These parameters describe the mechanical structure beneath Taiwan (e.g., Burov and Diament, 1995; Okaya et al., 1996).

3.1. Lithospheric integrated strength (LIS)

LIS represents the vertically integrated horizontal deviatoric stress needed to cause distortion, compression, or extension in the lithosphere (Artyushkov, 1973). It can be expressed as:

$$LIS = 2\int_0^L \tau(z)\mathrm{d}z \tag{3}$$

where $\tau(z)$ is the shear strength at depth z, and L is the thickness of lithosphere. Fig. 5 shows the total LIS in Taiwan orogenic belts and analyses the contribution to LIS from the different layers in the lithosphere. The total LIS for the hinterland is about 1.5×10^{12} N/m, which is only half of that for the foreland, 3×10^{12} N/m. The crustal strength contributes about 70% of the LIS in the foreland but up to 90% in the hinterland; while the lithospheric mantle strength contributes about 30% of the LIS in the former and only 10% in the latter. If we divided the crust into three layers as 0–15, 15–25, and 25 km Moho, the strength contributions of each layer to the LIS are similar at about 20–25% in the foreland. However, only 5% of the LIS

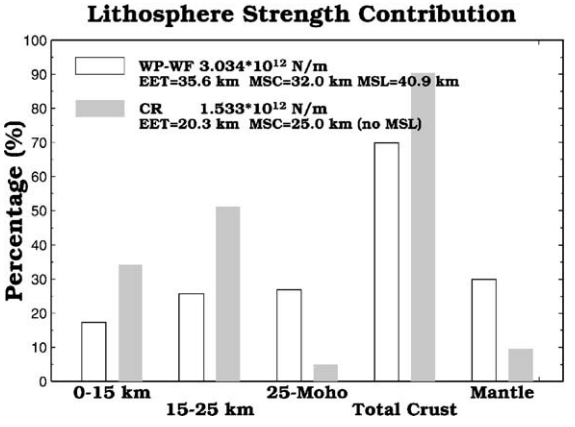

Fig. 5. Lithosphere strength contribution percentage from various depths for the foreland (WP–WF) and hinterland (CR). The mechanical strengths for foreland and hinterland are 3.034×10^{12} and 1.533×10^{12} N/m, respectively. The EET and the depth of the base of MSC and lithosphere (MSL) are also shown.

is within the range of 25 km Moho in the hinterland. Basically, the strength contribution from the upper 25 km in the crust is similar for both the foreland and the hinterland at about 1.3×10^{12} N/m. Below 25 km, however, the crustal strength of the foreland becomes about 10 times that of the hinterland. In addition, the lithospheric mantle strength in the foreland is also four to five times of that in the hinterland. These results imply that deep seismicity in the foreland reflects the strong lower crust and lithospheric mantle. On the contrary, a weak lower crust and lithospheric mantle preclude the occurrence of deep earthquakes in the hinterland.

3.2. MSC and MSL

In general, MSC and MSL indicate the regime of strong crust and strong lithosphere, respectively (e.g., Okaya et al., 1996). Critical shear strength, in general, could be taken as 250 bar to represent the lower bound of MSC and MSL (e.g., McNutt, 1984; Okaya et al., 1996). The shear strength of 250 bar is shown by a dashed line in Fig. 3. It shows that for a crustal thickness of 32 km, the crustal shear strength (MSC) exceeds the critical shear strength of 250 bar for depths of 5–32 km in the foreland, the lower depth of which corresponds to the 580 °C isotherm. In addition, the lithospheric shear strength (MSL) is over the critical shear strength up to depths of 41 km, which corresponds to the 750 °C isotherm. However, in the hinterland, the shear strength exceeds the critical shear strength only within the depth range of 5–25 km, due to its felsic bulk crust, The temperature at 25 km corresponds to the 450 °C isotherm. If we consider a critical shear strength in the range of 250 ± 50 bar, the depth of MSC and/or MSL and the corresponding temperatures will vary accordingly only within 2 km and 50 °C, respectively. The existence of a thick crust in the hinterland yields ductile deformation of dunite and mechanically weak lithospheric mantle. These temperatures are, in general, compatible to other studies (Burov and Diament, 1995; Cloetingh and Burov, 1996; Okaya et al., 1996). They show that the bottom of MSC is within the range of 300–500 °C isotherm and the bottom of MSL corresponds to 700–800 °C isotherm. If mafic granulite occurs in the lower crust, as the case of the foreland, the bottom of MSC could reach the 550 °C isotherm. In addition, the earthquake occurrences in Taiwan orogenic belts are in good agreement with the layers of MSC and MSL.

3.3. EET

The EET fundamentally shows the section of lithosphere that can accumulate tectonic stress. The EET of the oceanic lithosphere directly reflects its thermal structure and age. However, the EET of the continental lithosphere results from lithospheric lithology, loading distribution, and tectonic activities (e.g., Burov and Diament, 1995). When the crust and mantle are coupled, the EET is defined as (Burov and Diament, 1995):

$$EET = \sum_{i=1}^{n} h_i \tag{4}$$

When crust and mantle are decoupled, the EET is defined as (Burov and Diament, 1995):

$$EET = \sqrt[3]{\sum_{i=1}^{n} h_i^3} \tag{5}$$

where n represents the number of mechanically strong layers and h_i is the thickness of the ith layer of mechanically strong layers. The lithospheric shear strength profiles in Fig. 3 imply crust–mantle coupling in the foreland, but crust–mantle decoupling in the hinterland. Nevertheless, there is only one mechanically strong layer in the hinterland, which is about 20 km (5–25 km). The EET is about 20 km in the hinterland, which is about 40% less than that of about 36 km in the foreland, where three strong mechanically strong layers with thicknesses of about 20 km (5–25 km), 7 km (25–32 km), and 9 km (32–41 km) are found. Tectonic stresses, thus, can easily accumulate to cause large earthquakes in the foreland as documented in historical data (Tsai, 1985).

4. Discussion and conclusions

Our studies show a significant correlation of earthquake depth distributions to the thermo-mechanical structure beneath the young orogenic belt of Taiwan. We would like to further discuss the effect of

possible uncertainties, such as pore pressure, geotherm, and rheological stratification, on our previous results. We independently examine the temperature-vs.-earthquake cutoff depth (brittle/ductile transition) relationship. If we take D_{99} (the depth above which 99% of earthquakes occur) as the earthquake cutoff depth, the temperature-vs.-earthquake cutoff depth (brittle/ductile transition) relationship can be obtained. With a given specific composition, pore pressure, and D_{99}, the corresponding temperature to D_{99} can be obtained for the depth where brittle shear strength is the same as ductile shear strength (the location of brittle/ductile transition). Fig. 6a–d shows the brittle/ductile transition temperature for the RRs in the corresponding depth ranges as 5–15, 15–25, and 35–50 km, respectively. The curves are calculated from the condition of equality of the brittle and ductile strengths at the transition point. Two possible pore fluid pressures as 0.4 and 0.7 are considered. The D_{99} depths at the foreland and hinterland estimated from earthquake frequency–depth distribution are about 40 and 25 km, respectively. As shown in Fig. 6b and d, the temperatures at the depth of 40 and 25 km correspond to the values of 620–780 and 350–510 °C. The temperature derived from earthquake cutoff depth is compatible with geotherms of 750 and 450 °C. According to this evaluation, the earthquake cutoff depth as a geothermometer, as suggested by Bodri and Iizuka (1993), could not only provide the possible range of temperatures for the occurrence of seismicity, but also support our rheological model, although no direct laboratory rheological characteristics measurements are available for Taiwan.

From the relationship between brittle/ductile transition depth, temperature, and composition, we understand how temperature and composition simultaneously control the deformation style and seismicity within the crust and lithospheric mantle beneath the Taiwan orogenic belts. Considering the constitution of the crust, we constructed rheological models (stratifications) to evaluate the shear strength profiles and compared them with earthquake occurrence. Our results show that that mechanical structure is not necessary directly reflected in the thermal structure

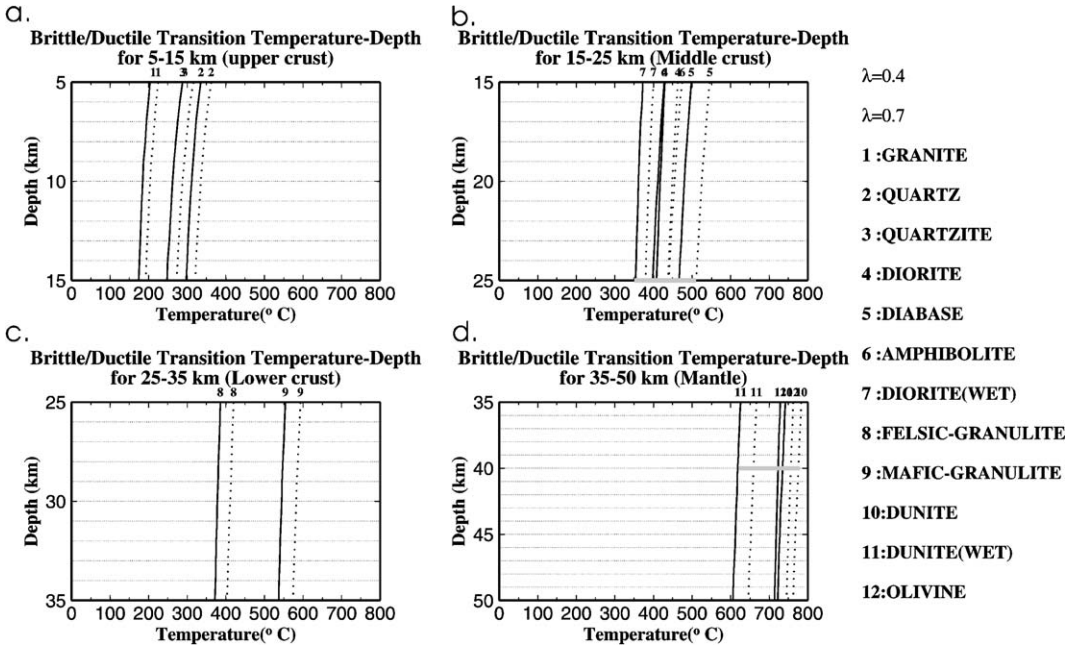

Fig. 6. Brittle/ductile transition temperature profiles for the RRs (represented by nos. 1–12) within depths of (a) 5–15 km, (b) 15–25 km, (c) 25–35 km, and (d) 35–50 km for pore pressures of λ=0.4 (solid) and λ=0.7 (dashed), respectively. The corresponding RR types to the numbers indicated above the curves are shown to the right of the figures. The horizontal gray bars in (b) and (d) show the yield temperature ranges corresponding to the D_{99} cutoff depth of 25 and 40 km for the hinterland and foreland.

as also suggested by Okaya et al. (1996). Our models demonstrate that two-layer seismicity can be attributed to the brittle layers in the foreland resulting from the moderate geotherm and intermediate–mafic bulk composition, while single-layer seismicity is due to felsic bulk composition in the hinterland. The results of our model predict that the MSC is not simply related to the thermal structure, as demonstrated by comparison of the MSC with crustal isotherm between 400 and 600°C and the surface heat flow. Compared to the strength profile developed by Mouthereau and Petit (2003), where the temperature at Moho is about 800–1000 °C, based on the high surface heat flow, our estimates of MSC, MSL, and EET give higher values. The results of Mouthereau and Petit (2003) postulate a weak mantle lithosphere in the foreland, whereas our model predicts a much stronger mantle lithosphere. This demonstrates that in active collision zones, a steady-state approximation of the thermal structure, which is parameterized by the surface heat flow, is not accurate enough to resolve the pattern of the deep mechanical structure. According to our model, in the foreland, MSC and MSL reflect frequent seismicity, if the tectonic stress exceeds the lithospheric shear strength. The shallow MSC in the hinterland is consistent with the upper 20–25 km seismicity. Weak lower crust and lithospheric mantle precluded the occurrence of deep earthquakes. In addition, the EET decrease from the orogenic margin (foreland) to the orogenic center (hinterland) is similar to the results of flexure modeling in Appalachians, Andes, Alps, and Himalayas (Stewart and Watts, 1997). Due to the weak LIS in the hinterland in Taiwan orogenic belts, crust thinning and rifting, in fact, could probably take place in the future as suggested by Teng (1996).

Acknowledgements

We thank two reviewers for their useful comments on the paper. Discussions with Dr. W.D. Mooney and during the SEISMIX2002 meeting were very helpful. We appreciate the seismic data provided by the Earthquake Center, Central Weather Bureau, Taiwan, ROC. This work was supported by NSC91-2119-M-008-014.

References

Artyushkov, E.V., 1973. Stresses in the lithosphere caused by crustal thickness inhomogeneities. J. Geophys. Res. 78, 7675–7708.

Bodri, B., Iizuka, S., 1993. Thermal regime, rheology and seismicity in Central Range. Tectonophysics 217, 1–9.

Burov, E.B., Diament, M., 1995. The effective elastic thickness (T_e) of continental lithosphere: what does it really mean? J. Geophys. Res. 100, 3905–3927.

Chen, C.H., Wang, C.H., Jeng, R.C., 1984. A preliminary study of the chemical composition of metapelites from the Central Range of Taiwan. Mem. Geol. Soc. China 6, 191–209.

Christensen, N.I., Mooney, W.D., 1995. Seismic velocity structure and composition of the continent crust: a global view. J. Geophys. Res. 100, 9761–9788.

Cloetingh, S., Burov, E.B., 1996. Thermomechanical structure of European continental lithosphere: constraints from rheological profiles and EET estimates. Geophys. J. Int. 124, 695–723.

Doser, D.I., Kanamori, H., 1986. Depth of seismicity in the imperial valley region (1977–1983) and its relationship to heat flow, crustal structure, and the October 15, 1979, earthquake. J. Geophys. Res. 91, 675–788.

Ho, C.S., 1988. An Introduction to the Geology of Taiwan Explanatory Text of the Geologic Map of Taiwan, 2nd edition. The Ministry of Economic Affairs, Republic of China, p. 192.

Kao, H., Shen, S.S., Ma, K.-F., 1998. Transition from oblique subduction to collision: earthquakes in the southernmost Ryukyu arc–Taiwan region. J. Geophys. Res. 103, 7211–7229.

Lamontagne, M., Ranalli, G., 1996. Thermal and rheological constraints on the earthquake depth distribution in the Charlevoix, Canada, intraplate seismic zone. Tectonophysics 257, 55–69.

Lee, C.R., Cheng, W.T., 1986. Preliminary heat flow measurement in Taiwan. Proceedings, 4th Circum-Pacific Energy and Mineral Resources Conference, Singapore, pp. 31–36.

Lee, C.Y., Chung, S.L., Chen, C.H., Hsieh, Y.L., 1994. Mafic granulite xenoliths from Penghu Islands: evidences for basic lower crust in SE China continental margin. J. Geol. Soc. China 36 (4), 351–379.

Lin, C.-H., 2000. Thermal modeling of continental subduction and exhumation constrained by heat flow and seismicity in Taiwan. Tectonophysics 324, 189–2001.

Lu, C.Y., Hsu, K.J., 1992. Tectonic evolution of the Taiwan Mountain belt. Petrol. Geol. Soc. China 27 (6), 21–46.

Ma, K.F., Song, D.R., 1997. Pn velocity and Moho depth in Taiwan. J. Geol. Soc. China 40, 167–184.

Ma, K.-F., Wang, J.-H., Zhao, D., 1996. Three-dimensional seismic velocity structure of the crust and uppermost mantle beneath Taiwan. J. Phys. Earth 44, 85–105.

Meissner, R., 1986. The Continental Crust: A Geophysical Approach. Academic Press, Orlando, FL, pp. 361–362. McNutt, M.K., 1984. Lithospheric flexure and thermal anomalies. J. Geophys. Res. 89, 11180–11194.

Mouthereau, F., Petit, C., 2003. Strength of the Eurasian continental lithosphere in the foreland of the Taiwan collision belt: constraints from seismicity, rheology, flexure and structure styles. J. Geophys. Res. 108, 2512.

Okaya, N., Freeman, R., Kissling, E., Mueller, St., 1996. A lithospheric cross-section through the Swiss-Alps: II. Constraints on the mechanical structure of a continent–continent collision. Geophys. J. Int. 127, 399–414.

Ranalli, G., 1995. Rheology of the Earth, 2nd ed. Chapman & Hall, London, p. 413.

Ranalli, G., Murphy, D.C., 1987. Rheological stratification of the lithosphere. Tectonophysics 132, 281–295.

Rau, R.J., Wu, F.T., Shin, T.C., 1996. Regional network focal mechanism determination using 3D velocity model and SH/P amplitude ratio. Bull. Seismol. Soc. Am. 80, 1270–1283.

Rudnick, R.L., Fountain, D.M., 1995. Nature and composition of the continental crust: a lower crustal perspective. Rev. Geophys. Space Phys. 33, 267–309.

Shih, R.C., Lin, C.H., Lai, H.L., Yeh, Y.H., Huang, B.B., Yen, H.Y., 1998. Preliminary crustal structures across central Taiwan from modeling of the onshore–offshore wide-angle seismic data. Terr. Atmos. Oceanic Sci. 9, 317–328.

Sibson, R.H., 1974. Frictional constraints on thrust, wrench and normal faults. Nature 249, 542–544.

Sibson, R.H., 1984. Roughness at the base of the seismogenic zone: contributing factors. J. Geophys. Res. 89, 5791–5799.

Song, T.-R.A., Ma, K.-F., 2002. Estimation of the thermal structure of a young orogenic belt according to a model of whole-crust thickening. Geol. Soc. Amer., 121–136.

Stewart, J., Watts, A.B., 1997. Gravity anomalies and spatial variations of flexural rigidity at mountain ranges. J. Geophys. Res. 102, 5327–5352.

Teng, L.S., 1990. Geotectonic evolution of late Cenozoic arc–continental collision in Taiwan. Tectonophysics 183, 57–76.

Teng, L.S., 1996. Extensional collapse of the northern Taiwan mountain belt. Geology 24, 949–952.

Tsai, Y.B., 1985. A study of disastrous earthquakes in Taiwan (1683–1895). Proceedings of the ROC–JAPAN Joint Seminar on Multiple Hazards Mitigation. National Taiwan University, Taipei, ROC, pp. 13–49.

Youh, C.C., Tan, L.P., 1975. Element distribution in the black shales and their metamorphic products along the South Cross-Island Highway, Taiwan. Proc. Geol. Soc. China 18, 17–28.

Yu, S.-B., Chen, H.-Y., 1994. Global positioning system measurements of crustal deformation in the Taiwan arc–continental collision zone. TAO 5, 477–498.

Wang, J.H., Chen, K.C., Lee, T.Q., 1994. Depth distribution of shallow earthquakes in Taiwan. J. Geol. Soc. China 37, 125–142.

Wu, F.T., Rau, R.-J., Salzberg, D.H., 1997. Taiwan orogeny: thin-skinned or lithospheric collision. Tectonophysics 274, 191–220.